

## Hydrothermal synthesis and characterization of uniform $\beta$ -Ga<sub>2</sub>O<sub>3</sub> hollow nanostructures by carbon nanospheres

B. K. Kang<sup>a</sup>, S. R. Mang<sup>b</sup>, K. M. Song<sup>a</sup>, K. S. Lee<sup>c</sup> and D. H. Yoon<sup>a, b, \*</sup>

<sup>a</sup>School of Advanced Materials Science & Engineering, Sungkyunkwan University, Suwon 440-746, Korea

<sup>b</sup>SKKU Advanced Institute of Nanotechnology (SAINT), Sungkyunkwan University, Suwon 440-746, Korea

<sup>c</sup>School of Information and Communication Engineering, Sungkyunkwan University, Suwon 440-746, Korea

This study examined the preparation of monoclinic  $\beta$ -Ga<sub>2</sub>O<sub>3</sub> hollow nanostructures with various firing temperatures ranging from 500 to 900 °C by using hydrothermal and calcination processes. The X-ray diffraction patterns indicate that  $\beta$ -Ga<sub>2</sub>O<sub>3</sub> hollow nanostructures were synthesized at temperatures over 600 °C. The Ga(OH)CO<sub>3</sub> components of the shell were confirmed by Fourier transform infrared spectrometry. An investigation with field-emission scanning electron microscopy indicated a white body color of  $\beta$ -Ga<sub>2</sub>O<sub>3</sub> hollow nanostructures at 800 °C with diameters of about 200 nm. However, the sample calcined at 500 °C showed brown body color and was not perfectly crystallized. The cathodoluminescence spectrum revealed blue emission at 300-500 nm, which was assigned to vacancies in  $\beta$ -Ga<sub>2</sub>O<sub>3</sub> hollow nanostructures.

**Key words:** Semiconductors,  $\beta$ -Ga<sub>2</sub>O<sub>3</sub>, Hollow nanostructures, FTIR.

### Introduction

In recent years, hollow micro-/nanostructures of metal oxide semiconductors (ZnO, In<sub>2</sub>O<sub>3</sub>, TiO<sub>2</sub>, Fe<sub>3</sub>O<sub>4</sub> and SnO<sub>2</sub>) with controlled size and shape have gained great attention in many areas, such as Dye-Sensitized Solar Cells (DSSCs), gas sensors, drug delivery systems, Li-ion batteries, and catalysts, due to their unique electronic and optical properties, low effective density, high specific surface area, and shell permeability [1-5]. Recently, hollow nanostructures have been made with various methods such as spray-drying, gas-blowing, template-directed synthesis, and colloidal templating synthesis [6-8]. Most of the semiconductor hollow nanostructures were fabricated with hard templates of carbon cores, because the carbon spheres could be made with micro-/nanosize, and their surface properties could be controlled. Additionally, multi-component precursors are attached easily to the modified surfaces of the carbon spheres [9-10].

Gallium oxide (Ga<sub>2</sub>O<sub>3</sub>) with  $\alpha$ -,  $\beta$ -,  $\gamma$ -,  $\delta$ -, and  $\epsilon$ -crystal structures is a promising candidate material for activation and passivation coatings [11], gas sensors [12], blue light emitters and luminescent phosphors [13], and photocatalysis [14]. Among these phases, the thermodynamically stable phase of the  $\beta$ -Ga<sub>2</sub>O<sub>3</sub> monoclinic structure, which has a wide band-gap of ~4.8 eV at room temperature, has received attention

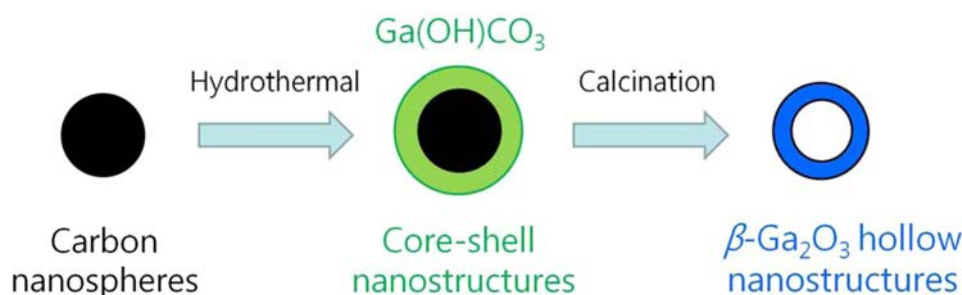
because it also has excellent chemical and thermal stability, electric conductivity, and luminescence properties, which depend on the native oxygen, gallium vacancies, and gallium oxide complex vacancies [15]. Despite the large number of reports on the synthesis of  $\beta$ -Ga<sub>2</sub>O<sub>3</sub> over the past few years, most reports focused on the synthesis of  $\beta$ -Ga<sub>2</sub>O<sub>3</sub> nanostructures such as nanowires, rods, and particles, which have been obtained with methods including vapor liquid solid (VLS), sol-gel, and hydrothermal method. These techniques have been attracting tremendous interest for their distinct advantages [16-18].

In the present work, highly uniform  $\beta$ -Ga<sub>2</sub>O<sub>3</sub> hollow nanostructures were successfully fabricated using carbon spheres as templates. We report on the synthesis, optical properties, and crystal morphology of blue-emission  $\beta$ -Ga<sub>2</sub>O<sub>3</sub> hollow nanostructures as a function of firing temperatures ranging from 500 to 900 °C.

### Experimental

In the typical synthesis of colloidal carbon spheres, glucose (10 g) was dissolved in 40 mL of distilled water to form a clear solution. The solution was then sealed in a 50-mL Teflon-lined stainless-steel autoclave and maintained at 170 °C for 6 hrs. The black-brown precipitates were washed with distilled water and ethanol three times and dried at room temperature in a vacuum oven. The  $\beta$ -Ga<sub>2</sub>O<sub>3</sub> hollow nanostructures were prepared by hydrothermal method using Ga(NO<sub>3</sub>)<sub>3</sub> · xH<sub>2</sub>O (99.9%, Sigma-Aldrich) and urea as the raw materials. The as-prepared carbon spheres (150 mg) were added and were well-dispersed into a mixed solvent of 48 mL

\*Corresponding author:  
Tel : +82-31-290-7388  
Fax: +82-31-290-7371  
E-mail: dhyoon@skku.edu



**Scheme 1.** Formation process for  $\beta$ -Ga<sub>2</sub>O<sub>3</sub> hollow nanostructures using carbon nanospheres as templates by hydrothermal method.

of ethanol and 8 mL of water with the assistance of sonication for 30 min. In the typical synthesis of the pure  $\beta$ -Ga<sub>2</sub>O<sub>3</sub> hollow nanostructures, 6 mmol (1.3544 g) of Ga(NO<sub>3</sub>)<sub>3</sub> · xH<sub>2</sub>O and 30 mmol (1.8 g) of urea were dissolved in the carbon colloid solution. Finally, the mixture was transferred to a 100-ml three-necked round flask and maintained at 90 °C for 48 h with vigorous stirring. After hydrothermal reaction, the products were washed with distilled water and ethanol three times. The washed precipitates were dried in a vacuum oven at room temperature for 24 hrs and finally calcined in air at 500 °C for 1 hr with a heating rate of 1 °C min<sup>-1</sup> and at 600–800 °C for 1 hr with a heating rate of 10 °C min<sup>-1</sup>.

The shape and morphology of the  $\beta$ -Ga<sub>2</sub>O<sub>3</sub> hollow nanostructures as a function of firing temperatures were observed by field-emission scanning electron microscopy (FESEM, JEOL 7500F). The crystallinity and structure of the  $\beta$ -Ga<sub>2</sub>O<sub>3</sub> hollow nanostructures were examined by powder X-ray diffraction (PDR-XRD, Bruker D8 FOCUS) using CuK $\alpha$  radiation. Fourier transform infrared spectroscopy (FTIR, Bruker IFS-66/S) was employed to analyze the chemical bonding within the materials. The thermogravimetry-differential thermal analysis (TG-DTA, Seiko Exstar) was measured in air at a heating rate of 5 °C/min from 30 to 900 °C to confirm the reaction of carbon spheres and crystallization of  $\beta$ -Ga<sub>2</sub>O<sub>3</sub> hollow nanostructures. The optical properties of the  $\beta$ -Ga<sub>2</sub>O<sub>3</sub> hollow nanostructures were analyzed using a room-temperature cathodoluminescence device (MONO CL3+, GATAN) with an excitation energy of 10 keV.

## Results and Discussion

Fig. 1 shows the XRD patterns of the  $\beta$ -Ga<sub>2</sub>O<sub>3</sub> hollow nanostructures after calcinations of Ga-coated core-shell nanostructures from 500 to 900 °C. The XRD patterns for  $\beta$ -Ga<sub>2</sub>O<sub>3</sub> at firing temperatures of 500 and 600 °C could barely be indexed because of the background peaks for the carbon of the core-shell structures and the low-intensity peaks of  $\beta$ -Ga<sub>2</sub>O<sub>3</sub> with a large full width at half maximum (FWHM). However, all diffraction patterns of the  $\beta$ -Ga<sub>2</sub>O<sub>3</sub> hollow nanostructures obtained with calcination at 700 °C were easily indexed to monoclinic crystalline  $\beta$ -Ga<sub>2</sub>O<sub>3</sub> (JCPDS

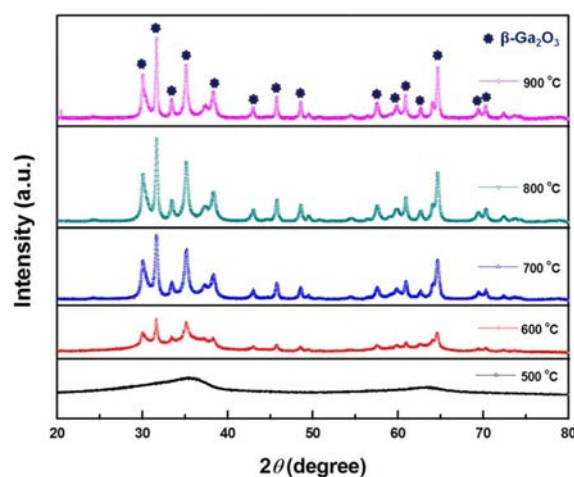


**Fig. 1.** XRD patterns of the calcined  $\beta$ -Ga<sub>2</sub>O<sub>3</sub> hollow nanostructures as a function of firing temperatures ranging from 500 to 900 °C for 1 hr.

Card 41-1103), with lattice parameters of  $a = 12.22$  Å,  $b = 3.038$  Å,  $c = 5.807$  Å, and  $\beta = 103.82$ . Various diffraction peaks for  $\beta$ -Ga<sub>2</sub>O<sub>3</sub> were observed, including those for the (400), (110), (401), (202), (002), (111), and (512) planes. The FWHM of the XRD peaks for the  $\beta$ -Ga<sub>2</sub>O<sub>3</sub> hollow nanostructures decreased with increasing firing temperature from 500 to 900 °C. This result indicates that the amorphous core-shell structures were perfectly crystallized after controlled calcination steps and increasing firing temperatures.

Fig. 2 shows the FTIR spectra in the region of 4000–400 cm<sup>-1</sup> of Ga-coated core-shell nanostructures and  $\beta$ -Ga<sub>2</sub>O<sub>3</sub> hollow nanostructures after calcination from 500 to 900 °C. The sharp and intense band absorption of Ga-coated core-shell structures was observed at 1384 cm<sup>-1</sup> due to the  $\nu_3$  mode of interlamellar [CO<sub>3</sub>]<sup>2-</sup> ions according to previous reports [19]. From these results, we think that all the chemical reactions of carbon@Ga(OH)CO<sub>3</sub> core-shell structures in a solution of water/ethanol and urea can be described as follows:



The results suggest that the component of the shell consists of Ga(OH)CO<sub>3</sub>. Strong absorption peaks

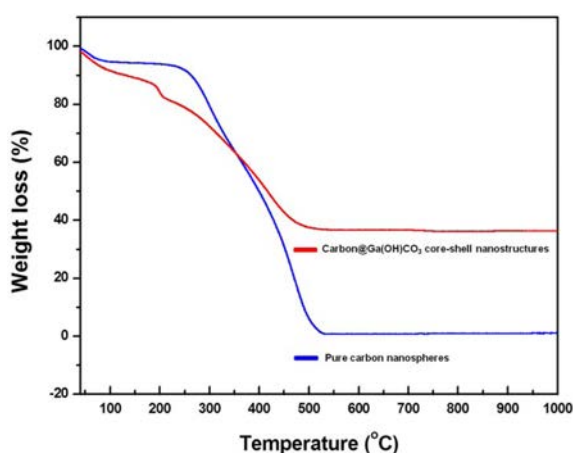


**Fig. 2.** TG curves of pure carbon nanospheres and carbon@Ga(OH)CO<sub>3</sub> core-shell nanostructure precursor in an open-air environment.

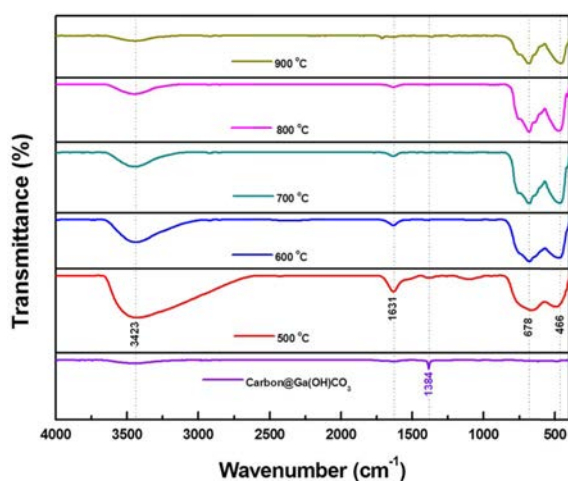


**Fig. 3.** FTIR spectra of carbon@Ga(OH)CO<sub>3</sub> core-shell nanostructures and  $\beta$ -Ga<sub>2</sub>O<sub>3</sub> hollow nanostructures as a function of firing temperatures ranging from 500 to 900 °C for 1 hr.

positioned at 466 and 678 cm<sup>-1</sup> (Ga-O stretching vibration) in Fig. 2 are identified in the  $\beta$ -Ga<sub>2</sub>O<sub>3</sub> hollow nanostructures obtained with calcination at temperatures over 600 °C for 1 hr [20]. Furthermore, the FTIR spectra show a broad absorption band of the -OH group (1631, 3436 cm<sup>-1</sup>), which results from the H<sub>2</sub>O absorbed by the  $\beta$ -Ga<sub>2</sub>O<sub>3</sub> hollow nanostructures when the samples were analyzed at room temperature in air [21].

Fig. 3 shows the thermal degradation patterns of the pure carbon nanospheres and carbon@Ga(OH)CO<sub>3</sub> core-shell nanostructures in air atmosphere. The TG reveals that during heating, the weight loss occurs in two steps of a slow loss of weight at 294 °C due to the dehydration and densification of carbon spheres, and a sharp loss of weight attributed to the burning of the carbon spheres (473 °C) [22]. Also, the weight loss of pure carbon template is nearly 100%. However, the residual weight percentage of the carbon@Ga(OH)CO<sub>3</sub> core-shell nanostructures is 36.3%, which was attributed

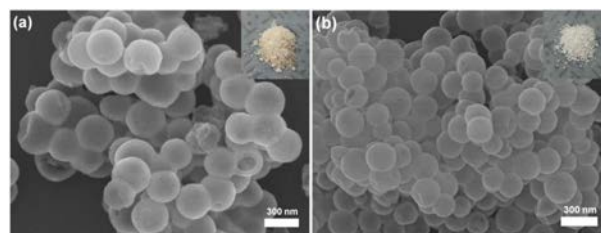


**Fig. 4.** FE-SEM images of the  $\beta$ -Ga<sub>2</sub>O<sub>3</sub> hollow nanostructures calcined at (a) 500 °C and (b) 800 °C for 1 hr. The insets show photographs of the  $\beta$ -Ga<sub>2</sub>O<sub>3</sub> hollow nanostructures calcined at 500 and 800 °C, respectively.

to crystallization and the formation of  $\beta$ -Ga<sub>2</sub>O<sub>3</sub> hollow nanostructures.

Figs. 4(a-c) show FE-SEM images of the pure carbon nanospheres prepared, the carbon@Ga(OH)CO<sub>3</sub> core-shell nanostructures, and pure  $\beta$ -Ga<sub>2</sub>O<sub>3</sub> hollow nanostructures obtained with calcination at 500 and 800 °C for 1 hr. As shown in Fig. 4(a), the pure carbon nanospheres have a uniform shape with a diameter of about 150-300 nm. The carbon@Ga(OH)CO<sub>3</sub> core-shell nanostructures maintain uniform spherical shape and appear to be monodispersed. However, the size and surface roughness of the carbon@Ga(OH)CO<sub>3</sub> core-shell nanostructures are larger and rougher than the pure carbon nanospheres, because the Ga atoms were deposited on the surface of the carbon nanospheres during the hydrothermal method. Figs. 4(c) and 4(d) show the FE-SEM images of  $\beta$ -Ga<sub>2</sub>O<sub>3</sub> hollow nanostructures obtained at firing temperatures of 500 and 800 °C, which indicate the formation of  $\beta$ -Ga<sub>2</sub>O<sub>3</sub> hollow nanostructures by the calcination process. The calcined samples consist of uniform and monodispersed hollow nanostructures with diameters of about 200-250 nm. This suggested that the slowly increased temperature during the calcination process causes slight shrinkage and sustains the shape and structure of the  $\beta$ -Ga<sub>2</sub>O<sub>3</sub> hollow nanostructures. However, the sample calcined at 500 °C shows brown body color, in contrast to the sample calcined at 800 °C, due to the residual carbon in  $\beta$ -Ga<sub>2</sub>O<sub>3</sub> hollow nanostructures.

Fig. 5 shows the CL spectra of  $\beta$ -Ga<sub>2</sub>O<sub>3</sub> hollow nanostructures as a function of the calcination temperatures ranging from 500 to 900 °C for 1 hr. A broad emission band from 400 to 600 nm was observed for sample calcined at temperatures over 600 °C. A strong blue emission peak was centered at approximately 450 nm. However, the  $\beta$ -Ga<sub>2</sub>O<sub>3</sub> hollow nanostructures show low emission intensity until the firing temperature of 600 °C is reached. This was attributed to the fact that the amorphous carbon @Ga(OH)CO<sub>3</sub> core-shell nanostructures were not perfectly crystallized. Furthermore, the blue emission of  $\beta$ -Ga<sub>2</sub>O<sub>3</sub> indicate the defect band emission by vacancies in the  $\beta$ -Ga<sub>2</sub>O<sub>3</sub> structure, such as gallium vacancies, oxygen vacancies, and gallium-oxygen vacancy pairs [23-24]. It was suggested that the emission peak originated from the recombination of an electron on a donor with a hole on

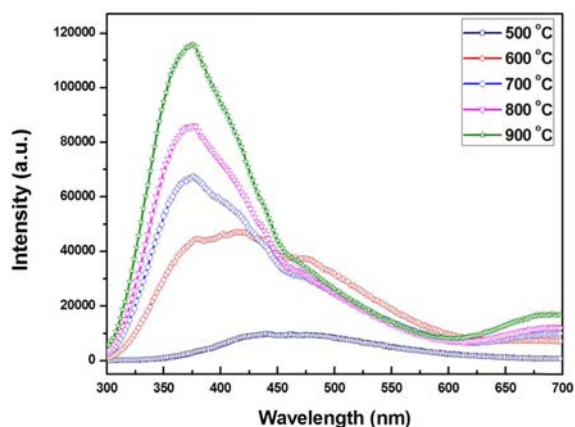


**Fig. 5.** Cathodoluminescence spectra of the  $\beta$ -Ga<sub>2</sub>O<sub>3</sub> hollow nanostructures as a function of firing temperatures ranging from 500 to 900 °C for 1 hr.

an acceptor formed by a gallium vacancy or gallium-oxygen vacancy pair in the  $\beta$ -Ga<sub>2</sub>O<sub>3</sub> crystal structures [23]. Also, with increasing firing temperatures, the blue shifted and increased luminescence peaks at 450 nm might be attributed to the improved crystal quality and increased oxygen vacancies in  $\beta$ -Ga<sub>2</sub>O<sub>3</sub> hollow nanostructures [25].

### Conclusions

In summary, we successfully synthesized  $\beta$ -Ga<sub>2</sub>O<sub>3</sub> hollow nanostructures by hydrothermal and calcination processes with various firing temperatures. The carbon @Ga(OH)CO<sub>3</sub> core-shell nanostructures calcined at 500 °C are amorphous, and the diffraction peaks of  $\beta$ -Ga<sub>2</sub>O<sub>3</sub> hollow nanostructures were increased as firing temperatures were increased up to 900 °C, because the crystallization is enhanced and the crystallite grows. The carbon@Ga(OH)CO<sub>3</sub> core-shell structures show sharp and intense band absorption at 1384 cm<sup>-1</sup> due to the  $\nu_3$  mode of the interlamellar [CO<sub>3</sub>]<sup>2-</sup> ions. Also, strong absorption peaks positioned at 466 and 678 cm<sup>-1</sup> (Ga-O stretching vibration) are identified in the  $\beta$ -Ga<sub>2</sub>O<sub>3</sub> hollow nanostructures. The blue shifted and increased luminescence peaks of samples calcined at temperatures ranging from 700 to 900 °C might be attributed to the improved crystal quality and increased vacancies in the  $\beta$ -Ga<sub>2</sub>O<sub>3</sub> hollow nanostructures.

### Acknowledgments

This research was supported by Basic Science Research

Program through the National Research Foundation of Korea (NRF) funded by the Ministry of Education, Science and Technology (NRF-2013R1A2 A2A01010027).

### References

1. Z. Dong, X. Lai, J.E. Halpert, N. Yang, L. Yi, J. Zhai, D. Wang, Z. Tang, and L. Jiang, *Adv. Mater.* 24 (2012) 1046-1049.
2. S. Liu, J. Yu, and S. Mann, *Nanotechnology* 20 (2009) 325606-325612.
3. S.-W. Cao, Y.-J. Zhu, M.-Y. Ma, L. Li, and L. Zhang, *J. Phys. Chem. C* 112 (2008) 1851-1856.
4. B. Li, Y. Xie, M. Jing, G. Rong, Y. Tang, and G. Zhang, *Langmuir* 22 (2006) 9380-9385.
5. X.W. Lou, Y. Wang, C. Yuan, J.Y. Lee, and L.A. Archer, *Adv. Mater.* 18 (2006) 2325-2329.
6. X.W. Lou, L.A. Archer, *Adv. Mater.* 20 (2008) 3987-4019.
7. S.-W. Kim, M. Kim, W.Y. Lee, and T. Hyeon, *J. Am. Chem. Soc.* 124 (2002) 7642-7643.
8. F. Caruso, R.A. Caruso, H. Möhwald, *Science* 282 (1998) 1111-1114.
9. M. Shang, W. Wang, H. Xu, *Cryst. Growth. Des.* 9 (2009) 991-996.
10. J. Yu, X. Yu, B. Huang, X. Zhang, Y. Dai, *Cryst. Growth. Des.* 9 (2009) 1474-1480.
11. M. Rebein, W. Henrion, M. Hong, J.P. Mannaerts, M. Fleischer, *Appl. Phys. Lett.* 81 (2002) 250.
12. R. Pohle, M. Fleischer, H. Meixner, *Sens. Actuators B* 68 (2000) 151.
13. C.H. Liang, G.W. Meng, G.Z. Wang, Y.W. Wang, L.D. Zhang, *Appl. Phys. Lett.* 78 (2001) 3202-3204.
14. Y. Hou, X. Wang, L. Wu, Z. Ding, and X. Fu, *Environ. Sci. Technol.* 40 (2006) 5799-5803.
15. L.-C. Tien, W.-T. Chen, C.-H. Hom, *J. Am. Ceram. Soc.* 94 (2011) 3117-3122.
16. K.W. Chang, and J.-J. Wu, *Adv. Mater.* 16 (2004) 545-549.
17. W.Y. Shen, M.L. Pang, J. Lin, and J. Fang, *J. Electrochem. Soc.* 152 (2005) H25-H28.
18. M. Ristix, S. Popovix, S. Musix, *Mater. Lett.* 59 (2005) 1227-1233.
19. L.S. Esteban, G.S. Mayela, R.G. Ma. Luisa, S. Isaac. J. *Porous Mat.* 3 (1996) 169-174.
20. U. Rambabu, N.R. Munirathnam, T.L. Prakash, B. Vengalrao, S. Buddhudu, *J. Mater. Sci.* 42 (2007) 9262-9266.
21. S.C. Vanithakumari, K.K. Nanda, *Adv. Mater.* 21 (2009) 3581-3584.
22. X. Sun and Y. Li, *Angew. Chem. Int. Ed.* 43 (2004) 3827-3831.
23. T. Harwig, J. Schoonman, *J. Solid State Chem.* 23 (1978) 205.
24. C.H. Liang, G.W. Meng, G.Z. Wang, L.D. Zhang, S.Y. Zhang, *Appl. Phys. Lett.* 78 (2001) 3202.
25. G. Sinha, S. Chaudhuri, *Mater. Chem. Phys.* 114 (2009) 644.